18.1

VORTICAL STRUCTURES IN CONVECTIVE BOUNDARY LAYERS AND IMPLICATIONS FOR THE INITIATION OF DEEP CONVECTION

Katharine M. Kanak
School of Meteorology, University of Oklahoma, Norman, Oklahoma

1. INTRODUCTION

The purpose of this study is to identify coherent structures in the convective boundary layer, in particular, vertical vortices of scales ranging from dust devil-scale to misocyclones-scale and to compare simulation results to observations.

Observations show that dust devils have been reported to be favored in environments characterized by little or no ambient winds (about less than 5 m s^{-1}; Webb 1963; Sinclair 1969). Morton (1966) states that wind speeds greater than 7-10 m s^{-1} will break up a dust devil. In addition, too much wind would modify (Moeng and Sullivan 1994) the cellular convective pattern to which the vertical vortices appear to be integrally tied (Willis and Deardorff 1979; Mason 1989; Kanak et al. 2000, hereafter KLS2000; Kanak 2005). The presence of mean winds or wind shears would provide a more obvious source of vorticity. So a more intriguing question is in such environments mean winds are negligible, from where does the vorticity come?

Results are presented from numerical simulations of the convective boundary layer (CBL) without imposed ambient winds that range from dust devil-scale O(10 m) up to a "parent cyclone"-scale, which in some cases is on the order of the misocyclone scale O(100) m. The relationship between these vortices, their structure and possible role in CBL processes will be presented.

2.METHODOLOGY

2.1. Numerical Model Description

The Kanak's System for Atmospheric Simulation (KANSAS) is a dry, three-dimensional, fully compressible, nonhydrostatic numerical model that integrates the Navier-Stokes equations. The model equations are presented in Kanak (1999) and are cast on an Arakawa C-grid. The velocity and scalar advection is represented by a second-order quadratic conserving "box" finite difference spatial scheme (Kurihara and Holloway 1967), The subgrid turbulence closure is a first-order Smagorinsky-Lilly (Smagorinsky 1962) scheme. A fourth-order numerical filter is employed. There are no prescribed mean ambient winds and the surface of the domain is heated with a constant flux condition. The lateral boundaries are periodic, and the upper and lower boundaries are rigid. The lower boundary is semi-slip.

2.2. Experiment Design

To explore the coherent structures for convective boundary layers, in particular vertical vortices, several numerical experiments have been carried out (Table I). For the vertical coordinate where more than one value is given for the grid spacing a vertically stretched coordinate has been used. It has been computationally impossible to date to model both the dust devil-scale and the misocyclone scale simultaneously, thus the problem has been separated into two parts. The first three simulations in Table 1 are larger-scale, coarser resolution simulations that are intended to examine the larger-scale vertical vortices, such as misocyclones, that arise in the cellular convective patterns themselves. The higher resolution simulations (6M, 2.75M and 2M) were designed to determine whether or not dust devil-scale vortices could be simulated with realistic observational physical characteristics. Vortices did form which generally compared well with observations (e.g. Kanak 2005).

	40M	35M	30M	6M	2.75 M	2M
$\Delta x = \Delta Y$	40	35	30	6	2.75	2
Δz	20	10.5-80.3	25	3-22	2.5-24	2. 1-24
Lx =Ly	5600	3000	4320	1004	1018	740
Lz	2000	2100	3600	1400	1200	1200

Table 1. Summary of numerical experiments

3. RESULTS AND DISCUSSION

3.1. Vertical Structure

Vertical vortices may be manifest as dust devils in the presence of a visible tracer, such as dust, although with the increase of remote sensing instrumentation, evidence of invisible vertical vortices is increasing (e.g., MacPherson and Betts 1997; KLS2000; Bos et al. 2005; Markowski and Hannon 2006). In some cases, smaller diameter dust devils are observed to be embedded within larger-scale "parent" circulations that are evident in observations (e.g., KLS2000, Markowski and Hannon 2006). This more complex vertical structure may be important in vertical transports of particulates to the free atmosphere. In addition, larger-scale vertical vortices, such as the parent cyclones, can be of misocyclone scale and in that case may have influence on deep convective initiation (e.g., Wilson et al. 1992; Kingsmill 1995; Lee et al. 2000; Pietrycha and Rasmussen 2004; Markowski and Hannon 2006; Arnott et al. 2006).

An example of a parent-scale vortex can be found in IHOP data. Figure 1 shows a horizontal plane of the vertical vorticity at 100 m height and the vertical velocity at 1000 m height (reproduced from Markowski and Hannon 2006). The white dashed line is a mesoscale convergence zone. Local vorticity centers that range from 1-4 km in diameter exist and these vorticity centers are said to have duration of 1-2 hrs. Numerous dust devils were reported on this date and near this time, but one in particular was reported to co-exist with one of the larger-scale vorticity centers (inside the white box).

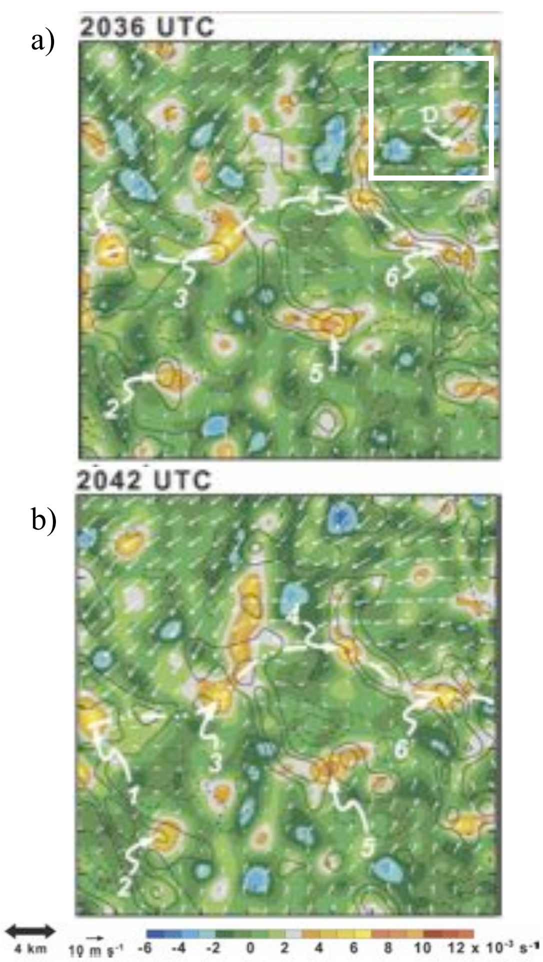

Fig. 1. XY Cross-sections of vertical vorticity (shaded) at 0.1 km and vertical velocity (contoured) at 1.0 km.

By the next time sampling (Fig. 1b), 6 min later, the dust devil was gone. This Fig. suggests that in some cases, the parent cyclones to dust devils may be the same thing as misocyclones. If so, this would provide a structural link between dust devils and larger-scale vortices.

What is the nature of this link or relationship between the small-scale dust devil vortex and the larger-scale parent/misocyclone? Sinclair (1966) presents the relationship using sailplane data (reproduced here as Fig. 2). In Fig. 2, the dust devil column is the very shallow narrow light grey shaded region in the lowest 100's of meters with a diameter of O(10) m. The disturbed airflow region, as denoted by departures in temperature and vertical velocity, extend well up into the boundary layer, even as high as three or more km and as wide as four km diameter (misocyclone scale). This Figure is a composite of data from 14 dust devils that have been corrected for vortex tilt and sailplane motion. This Figure represents a key point of this paper; that vortices with varying diameters exist in the CBL and may be responsible for important CBL processes such as vertical transports.

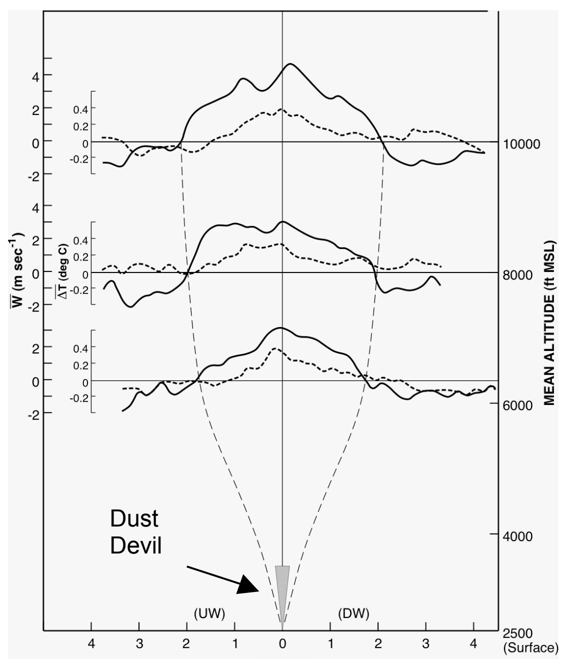

Fig. 2. (From Sinclair 1966). Composite data from 14 sailplane penetrations of dust devil's upper structure. Light grey shading denotes the height and width of a dust devil column near the surface. UW (DW) denotes upwind (downwind) of the dust devil based on translation direction. Disturbed wind field aloft has horizontal diameter up to 10 times that of the dust column.

Next, does a similar pattern appear in numerical simulations of the CBL? Figure 3 shows two XY panels of horizontal velocity vectors from the 40M simulation at 4140s and at a) z = 10 m and b) z =590

m. Here an anti-cyclonic vortex of about 100 m diameter exists at the low level and aloft, a 500 m vortex (misocyclone scale) of the same sign exists. The vortex is apparently broadened with height (similar to Fig. 2). Aloft there is considerably more swirling motion, but because it is spread over larger cross-sectional areas, the largest amplitudes of vertical vorticity are at the lowest model level.

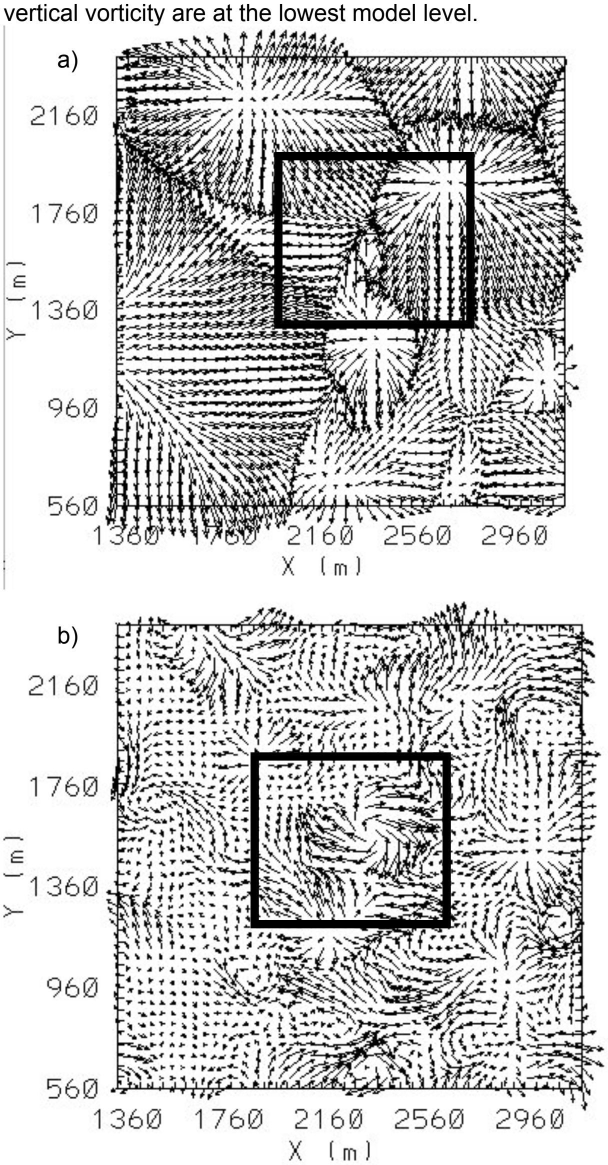

Fig. 3. 40M results, XY plane of horizontal velocity vectors at 4140s. a) at z = 10 m. Diameter of anti-cyclonic vortex is approximately 100 m. b) At z = 590 m. Diameter of broadened circulation is approximately 500 m.

Next the higher resolution simulations are examined to see whether or not vortices broaden with height in those simulations as well. Figure 4 shows horizontal velocity vectors from the 2.75M simulation. The diameter of the main anti-cyclonic vortex in Fig. 4a is approximately 19 m and there is significant cyclonic vorticity on periphery of the main anti-cyclonic vortex, particularly on the northeast side. This is a common feature observed by Sinclair (1973) and KLS2000. The maximum negative vertical vorticity amplitude is -1.4 s^{-1}.

At a height of 98 m (Fig. 4b), the horizontal velocity vectors show that the anti-cyclonic vortex has indeed broadened with height to a diameter of approximately 36 m. This is still considered a dust devil-scale vortex size. Perhaps a deeper domain might be required to allow this vortex to broaden further. The vorticity center has spread out laterally and the magnitude has decreased to –0.8 s^{-1}, likely owing to the available vertical vorticity being spread over a larger horizontal cross-section.

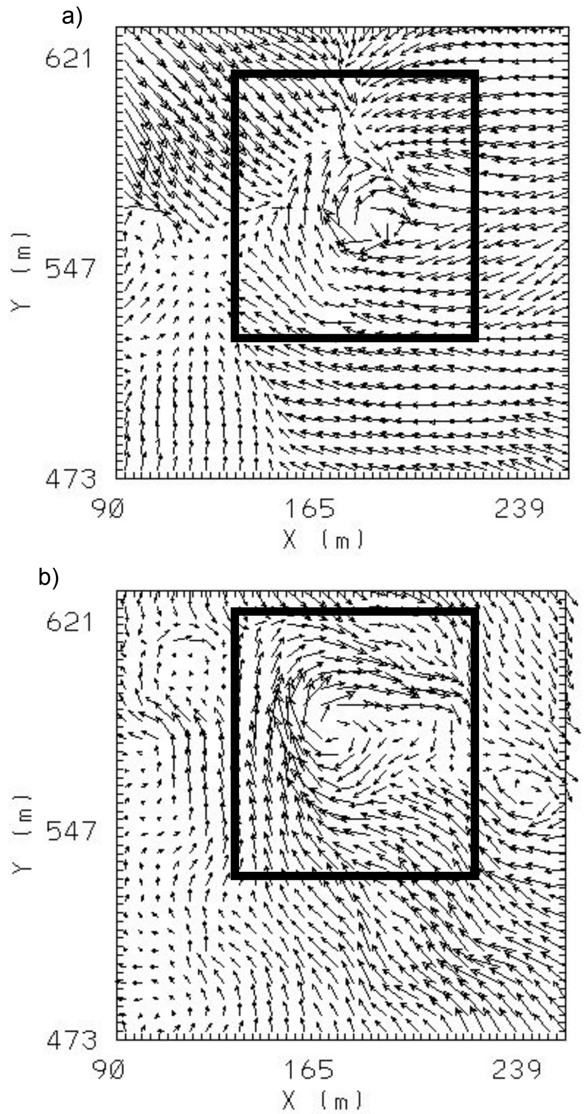

Fig. 4. 2.75M results, XY planes of horizontal velocity vectors at 1700s. a) at z = 2.5 m. Diameter of anti-cyclonic vortex is approximately 19 m. b) At z = 97.5 m. Diameter of broadened circulations is approximately 36 m.

Thus, dust devil-scale vertical vortices may be associated with misocyclone scale vortices aloft. Large eddy simulation has shown that misocyclones can form in the absence of mesoscale convergence zones, but rather in the cellular convective pattern itself. In addition, observations and simulations show that dust devil-scale vortices may be integrally tied to convective circulations that broaden with height and may influence CBL processes.

3.2. Coherent Structures and Vertical Transports

In 1988, Hunt et al. presented a schematic diagram (reproduced here as Fig. 5a,b) of the convective boundary layer. In particular, they showed a larger thermal updraft that extends over the depth of the boundary layer that included small shearing eddies and merging small plumes in the base of the thermal (Fig. 5a). Further idealization for the near surface region is given in Fig. 5b, in which the downdraft region (AD) is the broadest, and a more narrow updraft region (AU), which is fed by yet smaller diameter eddies near the surface. It is proposed that these smallest eddies may be rotating in some cases and that the simulation results are consistent with this schematic of the CBL. If it is true that helical flow inhibits mixing and thereby allows more efficient upward transport of heat and momentum (Andre and LeSieur 1977; Lilly 1986), then these small scale features may be more efficient at feeding the large-scale thermal updraft than non-rotating features.

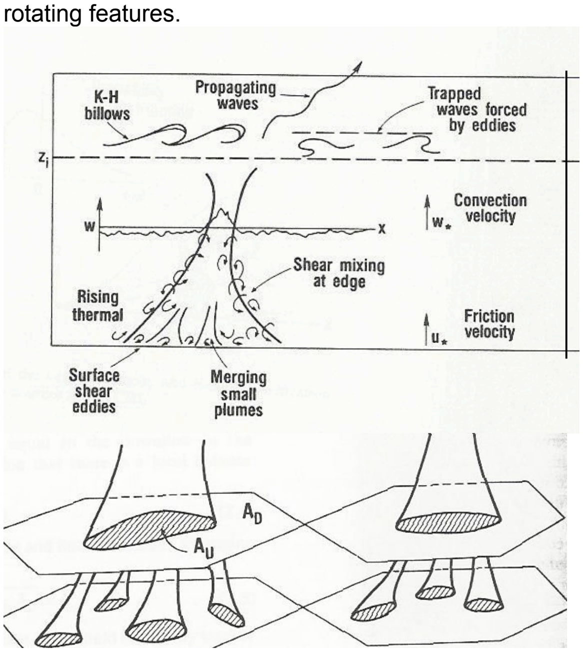

Fig. 5. (From Hunt et al. 1988). a) Schematic diagram of the flow and eddy structure of the convective boundary layer. b) Area of up (AU) and downdraft (AD) structure within thermals near the surface.

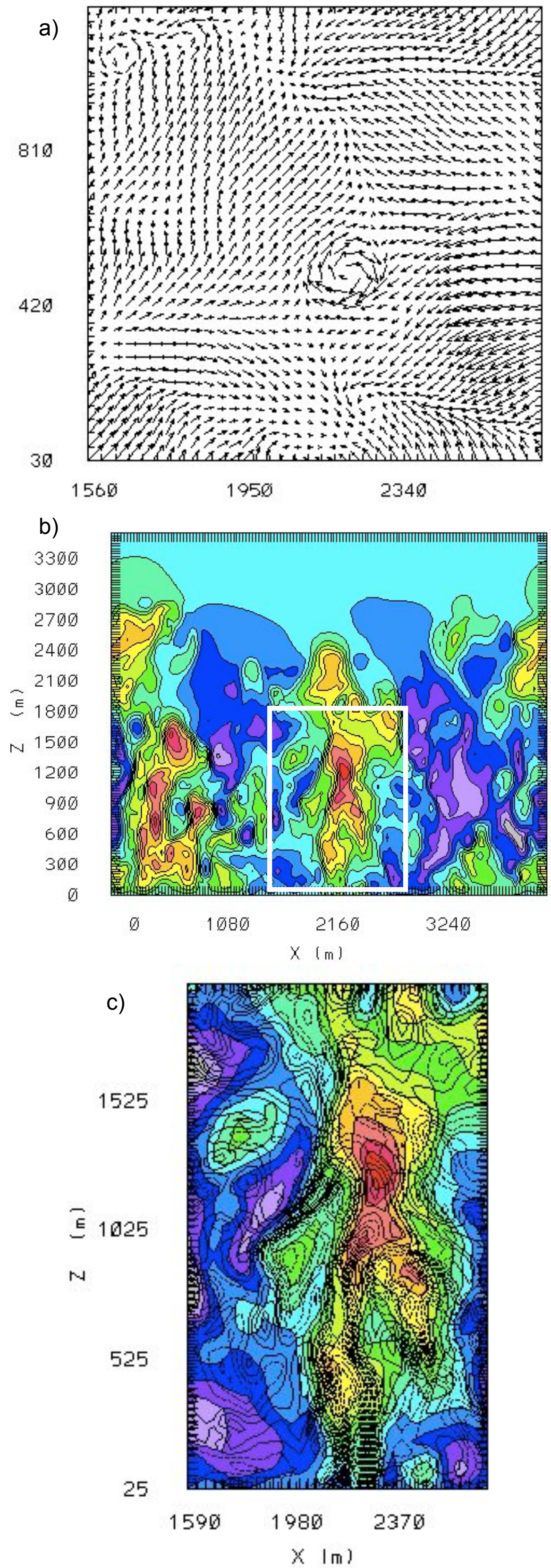

Fig. 6. 30M at 2500 s. a) XY subdomain plot of horizontal velocity vectors at z = 12.5 m. Maximum vector is 4.5 m s^{-1}. b) XZ of whole domain of w. Minimum value is –-5.1 m s^{-1}, maximum value is 7.2 m s^{-1} and interval is 0.88 m s^{-1}. c) inset of white box in b), w is shaded. Minimum value is –3.3 m s^{-1}, maximum value is 6.4 m s^{-1}, and the interval is 0.75 m s^{-1}. ζ contours in black. Minimum value is –0.19 s^{-1}, maximum value is 0.07 s^{-1}, and interval is 0.01 s^{-1}. The vertical coordinate is stretched for clarity.

Support for the enhancement of vertical heat transport in vertical vortices is shown in Fig. 6. Numerical simulations that employ coarser resolution are sometimes helpful in detecting coherent structures since they do not have as much small scale structure as higher resolution simulations. Thus, the 30M simulation is used to identify simulated structures that are similar to Fig. 5.

Figure 6a shows the XY cross-section of a subsection of the total domain of horizontal velocity vectors at z = 12.5 m in which there exists an anti-cyclonic vortex of approximately 300-400 m diameter (misocyclone size).

Figure 6b shows the vertical velocity in the XZ plane at t = 2500 s taken through the center of the vortex in Fig. 6a, in which there are two main updraft regions that extend to the top of the boundary layer (~2500-2700 m). The central plume outlined by the white box is the updraft of interest. Figure 6c shows a close-up view of the central updraft in the white box where shaded regions are vertical velocity and the overlain black contours are vertical vorticity. The vertical vorticity column is coincident with the strongest updraft regions. In this case, it is possible to say that the vortex is acting as a “feeder” to the updraft plume by moving heat away from the surface toward the top of the boundary layer.

3.3. Low Level Transects and Comparison with Observations

In low-level comparisons, Kanak (2005) showed that LES using 2 m horizontal resolution produced wind and temperature profiles that were qualitatively similar those of a particular vortex presented in Sinclair (1973) for a height of 2 m (not shown). At this height, and for a vortex of 5.2 m diameter, the temperature deviation was observed to be 5 K, the pressure deficit was 3 hPa, and the disturbance velocities were all on the order of 10 m s^{-1}. In the 2M (Fig. 7), for a vortex of 25 m diameter, the temperature increase was 3 K, and the wind amplitudes were on the order of those of Sinclair’s.

One difference between the simulation and observations is that the simulated pressure deficits were not as great in amplitude as the observed pressure deficits. A different lower boundary condition, such as constant temperature (instead of constant flux) could result in greater pressure deficits. This will be explored in future work. Both simulated and observed vortices exhibited weakened updraft cores within the vortex cores. It was also shown that the Burgers-Rott theoretical solution fit the high resolution simulated vortex data (Kanak 2005) better than the more often used Rankine vortex model (Fig. 7). This is important because as observational and numerical resolutions continue to increase, the data may be best represented by the Burgers-Rott vortex. To assume only the Rankine vortex may be misleading.

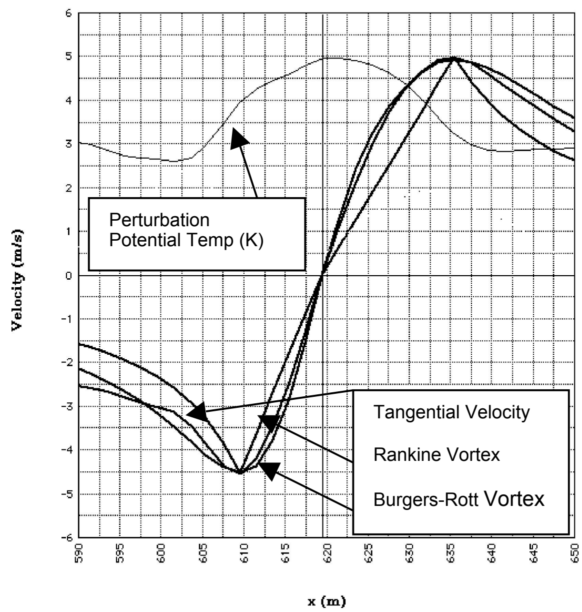

Fig. 7. For a vertical vortex in the 2MLES simulation, comparison of the Rankine and Burgers-Rott theoretical vortex solutions with a transect of the tangential velocity component, v, at t = 1100 s, z = 2.1 m, and y = 477 m. Also shown is the potential temperature deviation.

3.4. Horizontal Morphology

KLS2000 showed that the vertices of the cellular convective pattern that formed at low levels in the LESs were favored locations for the formation of parent-scale vertical vortices.. Note also that Willis and Deardorff (1979) found cell vertices to be favored locations for vertical vortex formation in a laboratory tank experiment. In both studies, cell vertices were regions of local vertical velocity maxima. In addition, several authors have documented that these horizontal open cell convective patterns exhibit a broadening in size with time. Figure 8 a shows the XY plane for the 6M simulation of the vertical velocity at time t = 300 s where the cell size is approximately 60 m in diameter. By 880 s (Fig. 8 b), the cell size is about 300 m or more.

The horizontal velocity vectors showed in all the simulations that multiple vortices were occurring simultaneously (after an initial spin up time, usually about 1000 s). An example is show in Fig. 9 for the 6M simulation where multiple vortices exists at time t

= 4030 s.

Figure 10 shows photographs of multiple dust devils occurring simultaneously near Corvallis, Oregon in July 2006 at about 1 pm local time and these were taken by Paul Naton (used with permission). These photos help support the simulation results in which multiple vortices are occurring at a given time. In addition, some fair weather cumulus can be observed in the vicinity of the dust devil fields and this is in contrast to the generally accepted opinion that clear skies are required for the formation of dust devils.

Animations of the horizontal velocity vectors at every 10 s and at the lowest model level, z = 3 m, for the 6M run show that vortices propagate along convergence zones, tend to circle about each other, and also tend to merge with vortices of the same sign or annihilate vortices of opposite sign. Note that Bluestein et al. (2004) also observed using radar that dust devils rotated around each other and they attributed this to the Fujiwara effect (1931).

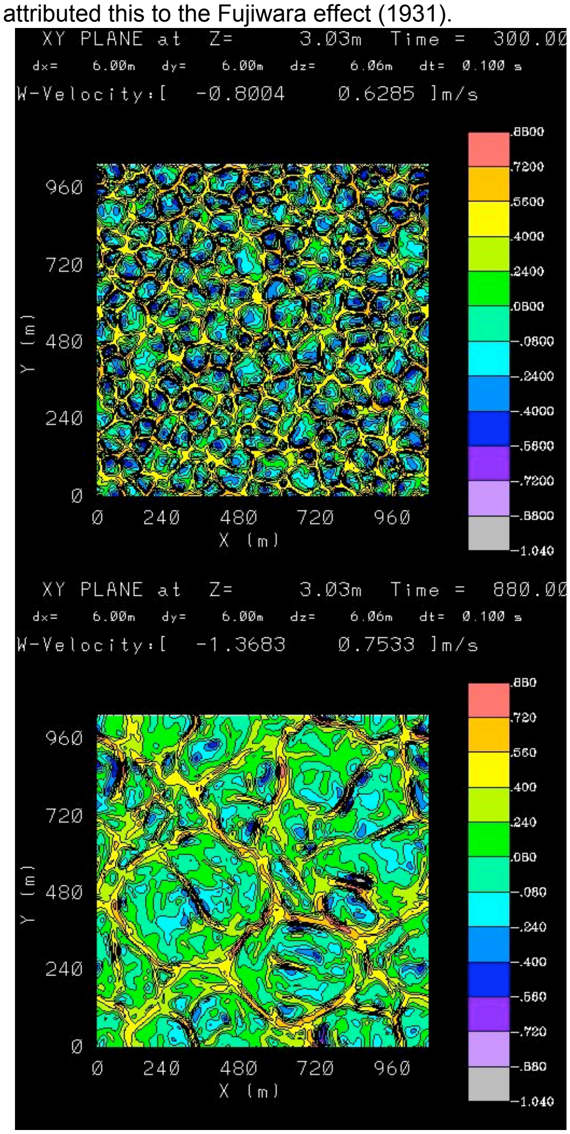

Fig. 8.XY Cross-sections of vertical velocity at z = 3 m for 6M simulation at a) 300s and b) 880 s.

Figure 11 shows the XY cross-sections of the vertical vorticity at the lowest model level z = 3m for the simulation 6M at (Fig.11a) t = 5900 s, (Fig. 11b) t = 5920 s, and (Fig. 11c) t = 6000 s. At 5900s, there are three anti-cyclonic centers that appear to draw closer to one another at 5920 s and at 6000 s they appear to merge. Meanwhile a cyclonic vorticity center to the northwest also appears to merge with smaller cyclonic centers and move toward the merged anticyclonic center. At the same time, the two oppositely signed vorticity centers appear to move around one another in behavior similar to that of misocyclones found during IHOP (Marquis et al. 2007). This behavior is most notable from animations of these fields.

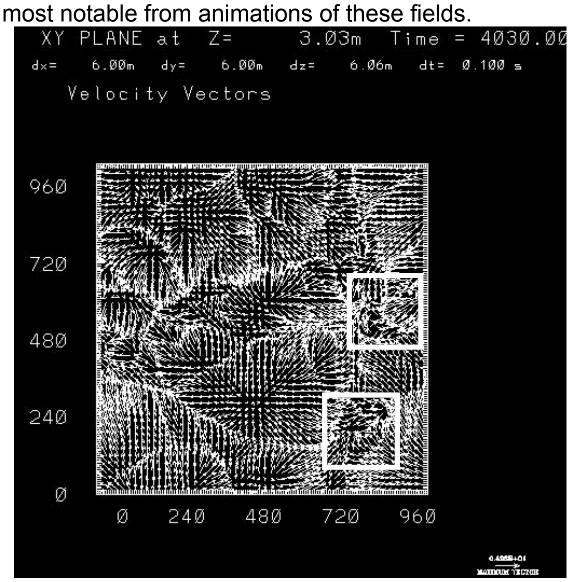

Fig. 9. XY Cross-sections of horizontal velocity vectors for 6M simulation, z = 3 m and time = 4030 s.

When the grid spacing of the LESs was reduced to 2.75 m and 2 m, vertical vortices were found not only at the cell vertices, but also embedded within the convergence branches that makeup the cellular pattern (Kanak 2005; her Fig. 2e-f). Note that Michaels and Rafkin (2004) also found this to be the case for their simulation of Martian dust devils. This "stairstep" behavior was also noted for misocyclones by several investigators (e.g. Marquis et al. 2007 and others). Figure 12 shows the stairstep pattern from a subsection of the 2.75M simulation. Figure 12a is the vertical velocity in the XY plane and Fig. 12 b shows the corresponding horizontal velocity vectors.

The Fig. from Kanak (2005) reproduced here as Fig. 13, which depicts a bookend vortex type pattern of very small dust devil size vortices, leads to at least two possible explanations for the existence of small-scale, near surface vertical vortices. First, is a conjecture put forth by Carroll and Ryan (1970) that downdrafts impinge on the surface and spread out in an asymmetric fashion, which is associated with horizontal shear, and thus vertical vorticity, on the

Fig. 10. Photos of multiple dust devils occurring near Corvallis, OR near 1 pm local time.

Used with permission from Paul Naton.

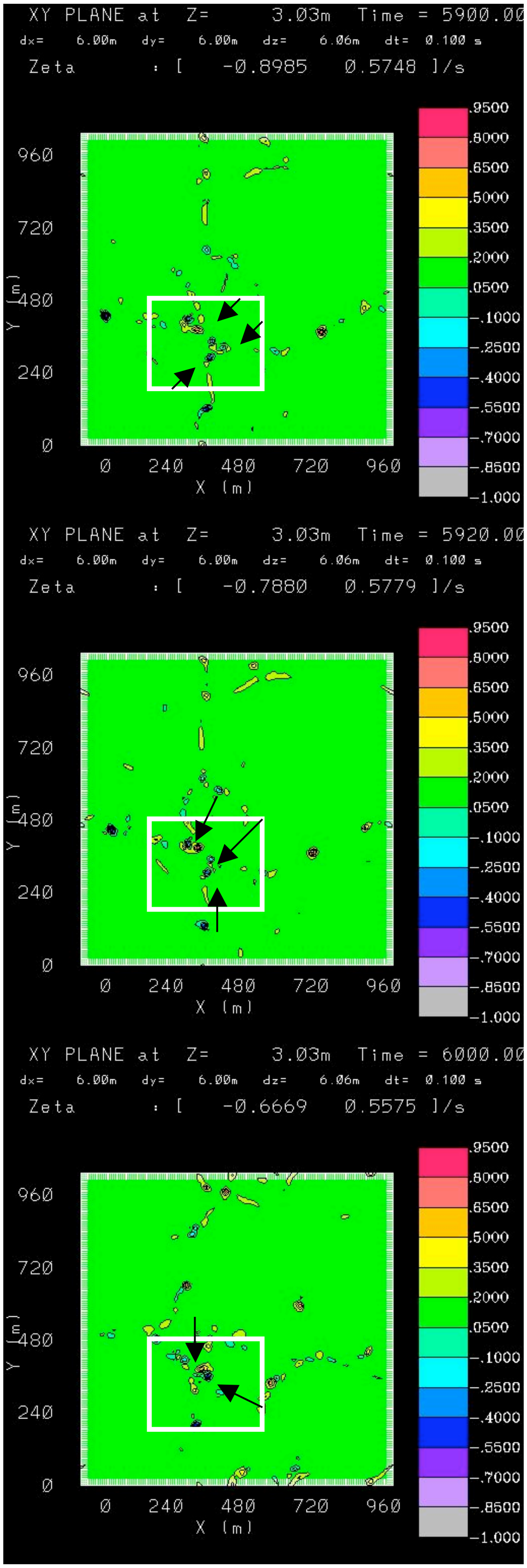

Fig.11. XY Cross-section of vertical vorticity for 6M at z = 3 m a) 5900s; b) 5920s, and c) 6000 s.

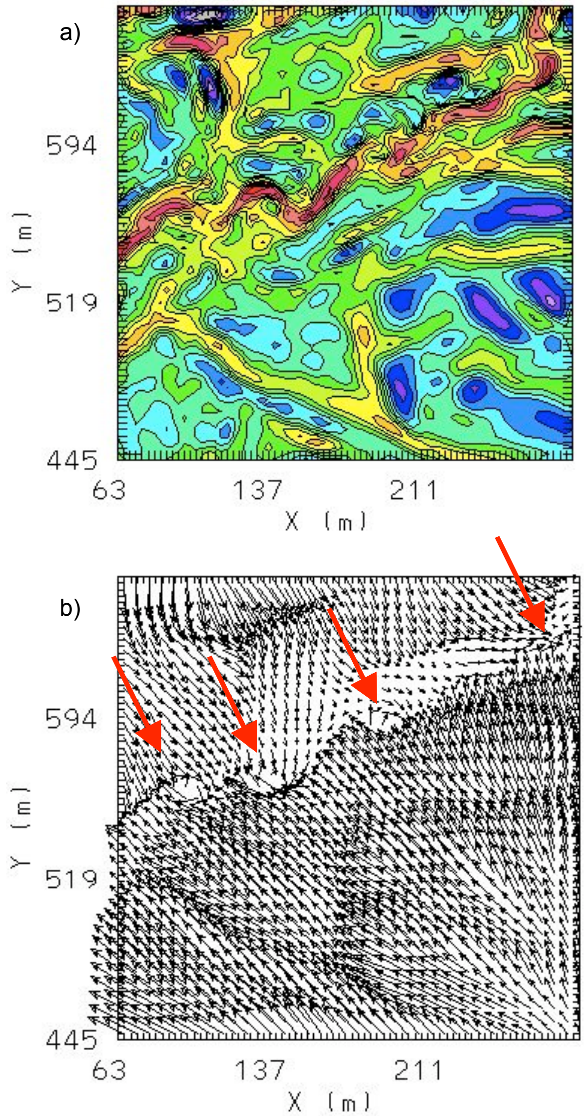

Fig. 12. 2.75M XY plane at z = 2 m and t = 1800 s. a) Vertical velocity (m s^{-1}). Minimum value is –0.86 m s^{-1}, maximum value is 0.89 m s^{-1} with interval 0.13 m s^{-1}. b) Horizontal velocity vectors. Vortices are denoted by red arrows

peripheries. Another possible explanation, is that horizontal vortex lines near the surface are tipped upward by the updrafts within the convergence zones and a hairpin vortex structure results (similar to that proposed by Church and Snow 1980 for firewhirls, their Fig. 9). Either scenario, and possibly other dynamical mechanisms, could explain the bookend vortex pattern.

4. SUMMARY AND CONCLUSIONS

A study of coherent structures is ongoing, particularly with regard to vertical vortices in the convective boundary layer that range from dust devil-scale to misocyclone scale vortices. Comparisons of numerically simulated structures to observations are made.

Owing to numerical constraints, the numerical task is divided into larger grid spacing (30-40m) simulations and smaller-scale grid spacing (2-6m) to examine each scale of motion.

Dust devil scale vortices are observed to be embedded within "parent-scale" cyclones, such as misocyclones.

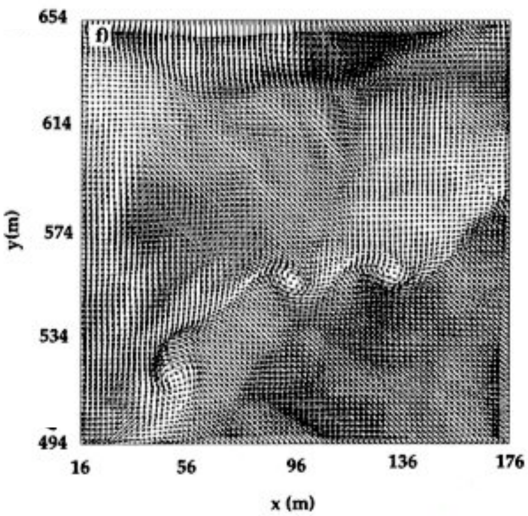

Fig. 13. From (Kanak 2005) 2M, horizontal velocity vectors in a bookend vortex pattern in a sub-domain at t = 1800 s and z = 2.1 m. Maximum velocity vector is 5 m s^{-1}.

Sinclair (1966) showed that wind fields were disturbed at distances of ten times the radius of dust devils and as high at 3 or more km. Both scales of simulations show broadening vertical vortices with height

Small-scale vortices may act as "feeders" into larger CBL plumes. This conceptual model put forth by Hunt et al. (1988) is found to be consistent with three-dimensional simulation results.

Low-level transects show that for simulations with the highest resolution, the Burgers-Rott theoretical vortex model better fits the data. In addition, the simulation results are consistent with the observations of Sinclair.

Horizontal planforms show cellular patterns that broaden with time and multiple vertical vortices that occur simultaneously. Photos provide observational evidence of multiple dust devils occurring in a single field simultaneously.

Vorticity centers propagate along convergence zones in the cellular convective pattern. In addition, they may move around one another or merge. Such behavior was observed in IHOP for misocyclone-scale vortices

Mechanisms, such as the roll-up of a vortex sheet (Barcilon and Drazin 1972), may lead to a stairstep pattern, and the tipping up of horizontal vorticity into hairpin vortices may result in a bookend vortex pattern.

Future work will include analyses to test such possible formation mechanisms for vertical vortices and further efforts to evaluate the effects of these vortices on CBL transports.

Acknowledgements: Thanks to Evgeni Fedorovich, Alan Shapiro and Jerry Straka for helpful discussions. Thanks also to Joan O'Bannon for her assistance with Fig. 2. Paul Naton provided the photos in Fig. 10. This work was supported by the National Science Foundation (NSF) ATM-0135510 and ATM-0733539.

REFERENCES

Andre, J. C., and LeSieur, M., 1977: Influence of helicity on high Reynolds number isotropic turbulence. *J. Fluid Mech.*, **81**, 187-207.

Arnott, N. R., Richardson, Y. P., Wurman, Y. P., and Rasmussen, E. N. 2006: Relationship between a weakening cold front, misocyclones, and cloud development on 10 June 2002 during IHOP. *Mon. Wea. Rev.*, **133**, 311-335.

Barcilon, A., and P. Drazin, 1972: *Dust devil formation*. Geophysical Fluid Dynamics Institute, Tech. Rept. 35, Florida State University.

Bluestein, H. B., Weiss, C. C. and Pazmany, A. L.,. 2004: Doppler radar observations of dust devils in Texas. *Mon. Weather Rev.*, **132**, 209–224

Bos, B. J., Gentry, B., Farrell, W. M., Jackson, T. L. Metzger, S., Comer, J. P. Dobler, J. McIntire, G. S., Neish, C., Smith, P. H., and Atlas, R., 2005: Dust Devil Observations from the 2005 MASST Field Experiment. Dust Devils on Earth and Mars: *Workshop. Sponsored by the ASU Planetary Geology Group, 19-20 September 2005*, U. S. Geological Survey Field Center, Flagstaff Arizona

Carroll, J. J., and Ryan, J. A., 1970: Atmospheric vorticity and dust devil rotation. *J. Geophys. Res.*, **75**, 5179-5184

Church, C. R. and Snow, J. T., 1980: Intense atmospheric vortices associated with a 1000 MW fire. *Bull. Amer. Meteor. Soc.*, **61**, 682-694

Fujiwara, S., 1931: Short note on the behavior of two vortices. *Proc. Phys. Math. Soc. Japan.*, **13**, 106-110.

Hunt, J. C. R., Kaimal, J. C., and Gaynor, J. E., 1988: Eddy structure in the convective boundary layer – new measurements and new concepts. *Quart. J. Roy. Meteor. Soc.*, **114**, 827-858

Kanak, K. M., 1999: "On The Formation Of Vertical Vortices In The Atmosphere". Ph.D. Dissertation, Univ. of Oklahoma, 204 pp.

Kanak, K. M., 2005: Numerical simulation of dust devil-scale vortices. *Quart. J. Roy. Meteor. Soc.*, **131**, 1271 – 1292.

Kanak, K. M., Lilly, D. K., and Snow, J. T., 2000: The formation of vertical vortices in the convective boundary layer. *Quart. J. of the Roy. Meteor. Soc.*, **126A**, 2789-2810

Kingsmill, D. E., 1995: Convection initiation associated with a seabreeze front, a gust front, and their collision. *Mon. Wea. Rev.*, 123, 2913-2933.

Kurihara, Y., and J. L. Holloway, 1967: Numerical integration of the nine-level global primitive equations model formulated by the box method. *Mon. Wea. Rev.*, **95**, 509-530.

Lee, B. D., Finley, C. A., and Wilhelmson, R. B., 2000: Simulating deep convection initiation by misocyclones. *Preprints 20th Conf. on Severe Local Storms*. Orlando, Amer. Meteor. Soc.

Lilly, D. K. 1986: The structure, energetics and propagation of rotating convective storms. Part II: Helicity and storm stabilization. *J. Atmos. Sci.*, **43**, 126-140

MacPherson, J. I., and Betts, A. K., 1997: Aircraft encounters with strong coherent vortices over the boreal forest. *J. Geophys. Res.*, **102, D24**, 29231-29234

Mason, P. J., 1989: Large-eddy simulation of the convective atmospheric boundary layer. *J. Atmos. Sci.*, **46**, 1492-1516.

Markowski, P. and Hannon, C., 2006: Multiple-Doppler radar observations of the evolution of vorticity extrema in a convective boundary layer. *Mon. Wea. Rev.*, 134, 355-374.

Marquis, J. N., Richardson, Y. R., and Wurman, J. M., 2004: Observations of misocyclones along boundaries during IHOP. *22nd Conference on Severe Local Storms.* Paper 16A.5.

Michaels, T. I. and Rafkin, S. C. R., 2004: Large eddy simulation of atmospheric convection on Mars. *Quart. J. of the Roy. Meteor. Soc.*, **130**, 1251-1275.

Moeng, C.-, H., and Sullivan, P. P., 1994: A comparison of shear- and buoyancy- driven planetary boundary layer flows. *J. Atmos. Sci.*, **51**, 999-1022.

Morton, B. R., 1966: Geophysical Vortices. Progress in Aeronautical Sciences, **7**, 145-193.

Pietrycha, A. E., and Rasmussen, E. N., 2004: Finescale surface observations of the dryline: a mobile mesonet perspective. *Wea. and Forecasting*, **19**, 1075–1088.

Sinclair, P. C., 1966: 'General characteristics of dust devils'. Ph.D. Dissertation, Univ. of Arizona, Tuscon.

Sinclair, P. C., 1969: General characteristics of dust devils. *J. Appl. Meteorol.*, **8,** 32-45

Sinclair, P. C., 1973: The lower structure of dust devils. *J. Atmos. Sci.*, **30**, 1599-1619

Smagorinsky, J. 1963: General circulation experiments with the primitive equations. I. The basic experiment. *Mon. Wea. Rev.*, **91**, 99-164.

Webb, E. K., 1963: Sink vortices and whirlwinds. *Proceedings of the 1st Australian Conference on Hydraulics and Fluid Mechanics*. Pergamon Press. Oxford.

Willis, G. E., and Deardorff, J. W., 1979: Laboratory observations of turbulent penetrative convection planforms. *J. Geophys. Res.*, **84**, 296-301.

Wilson, J. M., Foote, G. B. Crook, N. A. Fankhauser, J. C. Wade, C. G. Tuttle, J. D. and Mueller, C. K.,. 1992: The role of boundary layer convergence zones and horizontal rolls in the initiation of thunderstorms: A case study. *Mon. Wea. Rev.*, **120**, 1785-1815.